P H Y S I C A L   R E V I E W   L E T T E R S

Twist and Stretch of Helices Explained via the Kirchhoff-Love Rod Model of Elastic Filaments

Bojan Đuričković

Program in Applied Mathematics, University of Arizona, Tucson, Arizona AZ85721, USA

Alain Goriely

OCCAM, Mathematical Institute, University of Oxford, Oxford OX2 6GG, United Kingdom

John H. Maddocks

Section of Mathematics, Swiss Federal Institute of Technology (EPFL), Lausanne CH-1015, Switzerland
(Received 5 February 2013; published 5 September 2013)

In various single-molecule experiments, a chiral polymer, such as DNA, is simultaneously pulled and twisted. We address an elementary but fundamental question raised by various authors: does the molecule overwind or unwind under tension? We show that within the context of the classic Kirchhoff-Love rod model of elastic filaments, both behaviors are possible, depending on the precise constitutive relations of the polymer. More generally, our analysis provides an effective linear response theory for helical structures that relates axial force and axial torque to axial translation and rotation.

Single-molecule tweezer experiments have revealed many fascinating behaviors, some of which have been reported as counterintuitive. For instance, two different groups [1,2] measured the twist response of a single molecule of DNA when pulled by optical tweezers. In these beautiful experiments, a bead attached to the DNA is pulled by optical tweezers and the angular displacement is controlled via an applied torque. The experimental observations are that the DNA overwinds when pulled and extends when overwound. Both groups describe these behaviors as surprising: "simple intuition suggests that DNA should unwind under tension" [1], and "DNA should lengthen as it is unwound" [2]. We shall explain that the experimentally observed microscopic response is not particular to DNA and is in fact generic for most macroscopic helical elastic filaments. The behavior is captured by a simple 19th century model of helical wire confirmed experimentally more than a century ago [3,4].

Confusion on the sign of rotation also arises in the problem of growth of stems and roots where cell wall anisotropy is responsible for the overall handedness that is observed. A typical argument is that the cell wall is a cylindrical structure with reinforced, say, right-handed helical microfibrils, that rotates clockwise during growth (viewed from the top) [5,6], therefore unwinding, as expected, because "helices unwind when they are stretched" [7]. This explanation of handedness is again falsidical.

Before proceeding with our analysis, we discuss a possible rationale underlying the intuition in the above citations. If helical DNA or a plant is modeled by an elastic cylinder which remains cylindrical while stretched and twisted, then the simplest elastic energy [1,8,9] associated with deformations from the unstressed reference state is

$$E = \frac{1}{2}(A\theta^2 + 2B\theta z + Cz^2), \tag{1}$$

where $z = (L_1 - L_0)/L_0$ is the axial stretch (L_0 and L_1 being the initial and observed contour lengths), and θ is the rotational displacement of the end. The requirement that the energy be positive definite ($A > 0$, $C > 0$, $AC - B^2 > 0$) implies that a pure tension extends the spring and a pure axial torque twists the spring in the same direction, as expected. However, we show that, depending on the sign of B, the cylinder will either overwind or underwind when stretched at zero torque.

Further, experiments observe nonmonotonic behaviors at different loading regimes, which is not possible if the coefficients are constants. A nonlinear theory of rods is needed to derive the correct form of these energy functions.

The classic literature on helical rods concerns mostly the study of uniform helical metal springs with a circular cross section, cf. Fig. 1. Such systems were studied by Thomson and Tait (in Ref. [10], Sec. 605) who obtained the helical spring formulas (Love, Ref. [11], Sec. 271) which relate a wrench (M, N) (i.e., a prescribed axial torque and axial force both applied along the axis **e** of the helical spring, cf. Fig. 1) to the (constant) curvature κ and torsion τ of the resulting helical equilibrium

$$M = \epsilon[K_1\kappa(\kappa - \hat{\kappa}) + K_3\tau(\tau - \hat{\tau})]/\sqrt{\kappa^2 + \tau^2}, \tag{2}$$

$$N = \epsilon\sqrt{\kappa^2 + \tau^2}[K_3\kappa(\tau - \hat{\tau}) - K_1\tau(\kappa - \hat{\kappa})]/\kappa, \tag{3}$$

where $\hat{\kappa}$ and $\hat{\tau}$ are the (constant) curvature and torsion of the unstressed helical configuration $\epsilon = \pm 1$ if the spring is right- or left-handed, and K_1 and K_3 are the bending and torsional stiffnesses of the rod. The helical spring formulas imply that as tension $N > 0$ is increased monotonically
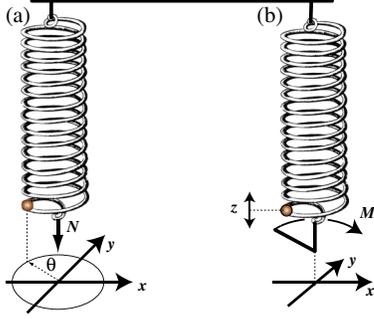
108103-1

FIG. 1 (color online).   A wrench applied to a helical spring gives rise to another helical equilibrium. Two simple questions are to determine (a) the sign of the increment of the rotation angle θ when an axial tension is applied with no torque and (b) whether a spring extends or contracts as a result of an axial torque loading with no applied force.

from zero at $M = 0$, the rotation first increases (overwinding the helical axis in the same direction as the reference handedness) and then decreases, returning to its initial value and then unwinding (cf. Fig. 2, right panel). This simple and quite general macroscopic behavior is no longer widely known and may therefore appear to be surprising and counterintuitive.

Modern molecular and biological experimental systems require a rod model with more general constitutive relations appropriate for filaments with noncircular cross sections and with coupling between bending and twisting strains. Here, we use a recent classification of all helical equilibria of such uniform filaments [12,13] to obtain an
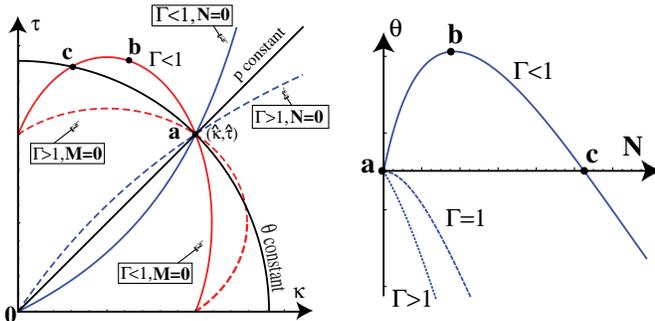

FIG. 2 (color online).   Left: For the particular constitutive relations (7), the set of $M = 0$ zero axial torque helical equilibria [corresponding to Fig. 1(a)] lie on an ellipse in the curvature-torsion plane determined by the value of Γ. Close to the unstressed helix with $N = 0$ (point **a**), $N > 0$ equilibria correspond to $|\tau| > |\hat{\tau}|$ (the case of $\tau > 0$ is shown). Initial overwinding in extension occurs for $\Gamma < 1$, which is when the section of the ellipse outside the circle centered at the origin and passing through **a** has $|\tau| > |\hat{\tau}|$. The set of $N = 0$ zero force equilibria [corresponding to Fig. 1(b)] is also shown. Depending on Γ, the helix either lengthens when wound ($\Gamma < 1$) or shortens ($\Gamma > 1$). Right: For $M = 0$, the relative coiling angle as a function of the axial force. For $\Gamma < 1$ and $N > 0$, the helix first overwinds, then unwinds.

effective response theory relating the two generalized loadings of axial force and axial torsion to the two generalized displacements of axial translation and axial rotation. We systematically derive the appropriate version of the effective helical energy (1) for general elastic rods and the associated generalized helical spring formulas, and we show that helical equilibria may initially either overwind or underwind when stretched, with the response dependent upon the detail of the loading and the constitutive relations.

We first summarize the Kirchhoff theory of inextensible, unshearable, uniform rods with quadratic strain-energy density [11,14]. A rod with arc length $s \in [0, L]$ is defined by a centerline $\mathbf{r}(s)$ and a unit vector field $\mathbf{d}_1(s)$ perpendicular to $\mathbf{r}'(s) =: \mathbf{d}_3(s)$ (the prime denotes the s derivative). A local orthonormal basis of directors is obtained by defining $\mathbf{d}_2(s) := \mathbf{d}_3(s) \times \mathbf{d}_1(s)$. This director basis is related to the classic Frenet basis formed from the principal normal $\boldsymbol{\nu}$, binormal $\boldsymbol{\beta}$, and tangent $\boldsymbol{\tau} = \mathbf{d}_3(s)$ vectors by $\mathbf{d}_1 = \boldsymbol{\nu} \cos\varphi + \boldsymbol{\beta} \sin\varphi$ and $\mathbf{d}_2 = -\boldsymbol{\nu} \sin\varphi + \boldsymbol{\beta} \cos\varphi$, where φ is an angle defining the rotation of the vector $\mathbf{d}_1$ in the normal plane. Since the vectors $\mathbf{d}_i$ form an orthornormal basis, their derivatives are $\mathbf{d}_i' = \mathbf{u} \times \mathbf{d}_i$, $i = 1, 2, 3$, where $\mathbf{u}$ is the Darboux vector, related to the curvature $\kappa \geq 0$, the (geometric) torsion τ, and the angle φ by $\mathbf{u} = \kappa \sin\varphi \mathbf{d}_1 + \kappa \cos\varphi \mathbf{d}_2 + (\tau + \varphi')\mathbf{d}_3$. The constitutive relations of an elastic filament must be written in the local basis. We write $\mathbf{u} = u_1 \mathbf{d}_1 + u_2 \mathbf{d}_2 + u_3 \mathbf{d}_3$ with the three components assembled into a triple $\mathbf{u} = (u_1, u_2, u_3)$ (note the use of sans-serif fonts for components in the director basis, which is a standard notation in the modern elasticity literature [14]). By defining a resultant force $\mathbf{n}(s)$ and moment $\mathbf{m}(s)$ acting on the cross section at $\mathbf{r}(s)$, and in the absence of distributed body forces and couples, the equilibrium equations are $\mathbf{n}' = \mathbf{0}$ and $\mathbf{m}' + \mathbf{d}_3 \times \mathbf{n} = \mathbf{0}$ which read in the local basis

$$\mathbf{n}' + \mathbf{u} \times \mathbf{n} = \mathbf{0}, \tag{4}$$

$$\mathbf{m}' + \mathbf{u} \times \mathbf{m} + \mathbf{v} \times \mathbf{n} = \mathbf{0}, \qquad \mathbf{v} := (0, 0, 1)^T. \tag{5}$$

A wrench is defined with respect to a given fixed axis $\mathbf{e}$ as $N := \mathbf{n} \cdot \mathbf{e} = \mathbf{n} \cdot \mathbf{e}$, $M := \mathbf{n} \cdot \mathbf{e} = \mathbf{m} \cdot \mathbf{e}$. The general material response of a rod with quadratic energy is given by a linear constitutive relation

$$\mathbf{m} = \mathbf{K}(\mathbf{u} - \hat{\mathbf{u}}), \qquad \mathbf{K} = \begin{pmatrix} K_1 & 0 & K_{13} \\ 0 & K_2 & K_{23} \\ K_{13} & K_{23} & K_3 \end{pmatrix},$$
$$K_1 \leq K_2, \tag{6}$$

where $\hat{\mathbf{u}}$ are the Darboux components of the unstressed shape (assumed constant), and $\mathbf{K}$ is positive definite.

Classic case.—Thompson, Tait, and Love consider the special case in which the constitutive relations (6) are

$$\mathbf{K} = \mathrm{diag}(K_1, K_1, K_3), \qquad \hat{u}_1 = 0, \qquad \Gamma := K_3/K_1. \tag{7}$$

Then, as shown, for example, in Ref. [15], the only possible helical equilibria have $u_1 = 0$, $u_2 = \kappa$, and $u_3 = \tau$ with the rod loaded by a wrench (M, N) along its helical axis. By using Eqs. (6) and (7) in Eqs. (4) and (5), the helical spring formulas (2) and (3) are obtained. If we further specialize our problem to the case where there is no torque $M = 0$, Eq. (2) reduces to a quadratic condition on the curvature κ and torsion τ independent of the loading:

$$\kappa(\kappa - \hat{\kappa}) + \Gamma\tau(\tau - \hat{\tau}) = 0. \tag{8}$$

We define the coiling angle per unit arc length to be $\rho = |\mathbf{u}|$, so that in the unstressed state, $\hat{\rho} = |\hat{\mathbf{u}}|$. Close to the unstressed state, we can then express the axial stretch $z = \tau/\rho - \hat{\tau}/\hat{\rho}$ and rotation angle $\theta = \rho - \hat{\rho}$ as a function of N:

$$z = \frac{(K_1\hat{\kappa}^4 + K_3\hat{\kappa}^2\hat{\tau}^2)}{K_1 K_3(\hat{\kappa}^2 + \hat{\tau}^2)^3}N + O(N^2), \tag{9}$$

$$\theta = \frac{(K_1 - K_3)\hat{\kappa}^2\hat{\tau}}{K_1 K_3(\hat{\kappa}^2 + \hat{\tau}^2)^2}N + O(N^2). \tag{10}$$

The first equation gives the linear approximation at the origin to the graph in Fig. 2(b), which demonstrates that a helix will initially overwind when pulled from its minimum energy state if and only if $\Gamma < 1$. We remark that if the filament is formed from a three-dimensional homogeneous linearly elastic material with Poisson ratio in [0, 1/2], e.g., standard metals, then $\Gamma \in [2/3, 1]$, so that initial overwinding in response to positive tension always arises for simple helical springs, a slightly surprising but yet completely classic effect. Equation (9) defines an effective Hooke constant for small extension.

Geometrically, Eq. (8) describes an ellipse in the curvature-torsion plane, which allows us to move beyond the linear analysis. For given material parameters Γ, $\hat{\kappa}$, and $\hat{\tau}$, all $M = 0$ helical solutions lie on this ellipse and the helix always extends when pulled (that is, $|\tau| > |\hat{\tau}|$ for $N > 0$). A point on the ellipse corresponds to overwound configurations with respect to $(\hat{\kappa}, \hat{\tau})$ when it lies outside the circle centered at the origin and of radius $\hat{\rho}$. It follows that for $N > 0$, a helix will initially overwind when pulled from rest if and only if $\Gamma < 1$. Further, the maximum overwinding (point **b** in Fig. 2) is obtained when the ellipse (8) intersects the hyperbola $2(1 - \Gamma)\kappa\tau + \Gamma\hat{\tau}\kappa - \hat{\kappa}\tau = 0$, and the coiling angle returns to its original value when the ellipse reintersects the circle $\rho^2 = \hat{\rho}^2$ (corresponding to the point **c**).

Analogously, we can study the particular loading $N = 0$ when a helix is subject to a pure axial torque $M \neq 0$, corresponding to the experiment in Fig. 1(b). Again, an analysis of the relative position of the level set curve $N = 0$

with respect to both the circle passing through the unstressed state (constant angle θ) and the line through the unstressed state and the origin (constant pitch p) reveals that for $\Gamma < 1$, initially unstressed helices always extend when overwound and shorten when unwound.

General case.—For the general constitutive laws (6), all helical equilibria can still be classified [12,13]. Generically, there are helical equilibria with both the Darboux vector $\mathbf{u}$ and $\mathbf{u}$ constant. Curvature, torsion, and radius are given by $\kappa = \sqrt{u_1^2 + u_2^2}$, $\tau = u_3$, and $R = \kappa/|\mathbf{u}|^2$. Let $\mathbf{e} = \epsilon\mathbf{u}/|\mathbf{u}|$ be a unit vector along the helical axis such that $\mathbf{e} \cdot \mathbf{r}'(s) \geq 0$, with $\epsilon = +1$ for right-handed helices and $u_3 = \tau \geq 0$ ($\epsilon = -1$ for left-handed helices). The pitch per unit arc length along $\mathbf{e}$ is $p = |u_3|/|\mathbf{u}|$ with the number of helical periods being $L\rho/2\pi$ for a helix segment of arc length L (with $\rho = |\mathbf{u}|$ as before). When one helical configuration is deformed into another, it will overwind if $\theta := \rho_2 - \rho_1 > 0$ and unwind if $\theta < 0$ (respectively, increasing or decreasing the number of helical repeats for a given arc length). The constant triples $\mathbf{u}$ in Darboux space lie on a quadric $\mathcal{Q}(\mathbf{u}) = 0$ (see the Supplemental Material [16]). This quadric (apart from degenerate cases, including the classic case discussed above in which the quadric degenerates to a plane) is a one-sheeted hyperboloid (see Fig. 3). Similarly, the wrench (M, N) defines two other manifolds in Darboux space, given by the level sets of $\mathcal{N}(\mathbf{u}) := N = \mathbf{n} \cdot \mathbf{e} = \epsilon\mu|\mathbf{u}|$ and $\mathcal{M}(\mathbf{u}) := M = \mathbf{m} \cdot \mathbf{e} = \epsilon\mathbf{u} \cdot \mathbf{m}/|\mathbf{u}|$, where $N\mathbf{e} = \mathbf{n}(L)$ and $M\mathbf{e} = \mathbf{m}(L) - N\mathbf{r}(L) \times \mathbf{e}$.

We now have a purely geometric problem: for a given wrench (M, N), the observed response (p, ρ) is determined by the intersection of the level sets of the functions $\mathcal{N}(\mathbf{u})$ and $\mathcal{M}(\mathbf{u})$ with the hyperboloid $\mathcal{Q}(\mathbf{u}) = 0$. It is these intersections of level sets which provide the generalized helical spring formulas, but now the explicit expressions
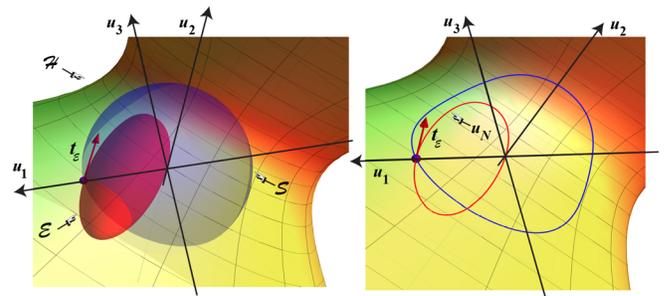

FIG. 3 (color online). Left: The set of equilibria for a helix under pure axial force ($M = 0$) is the intersection of the hyperboloid $\mathcal{H}$ (yellow region) and the ellipsoid $\mathcal{E}$ (red region). The set of equilibria without winding $\theta = 0$ is the intersection of the hyperboloid $\mathcal{H}$ (yellow region) and the sphere $\mathcal{S}$ (blue region). Right: For the particular case shown, the helix initially unwinds when pulled since the tangent $\mathbf{t}_{\mathcal{E}}$ to the curve of equilibria $\mathbf{u}_N$ (red curve) oriented toward $N > 0$ lies within the sphere $\mathcal{S}$, whose intersection with $\mathcal{H}$ is shown as the blue curve.

are not simple. Nevertheless, we can reconsider the problem of rotation in pure axial force close to the unstressed $N = M = 0$ helix $\hat{\mathbf{u}}$: does a helix over- or underwind for $M = 0$ and $N > 0$ and small? The required argument is in essence the same as the one in the (κ, τ) plane but now on the quadric $\mathcal{Q}(\mathbf{u}) = 0$ embedded in three-dimensional Darboux space. The condition $M = 0$ restricts the solutions to lie on the intersection of the quadric $\mathcal{Q} = 0$ with an ellipsoid $\mathcal{E} = 0$ (shown in red in Fig. 3) that generalizes the ellipse obtained in the classic case. Through the use of this geometric approach (see details in the Supplemental Material [16]), the explicit and general criteria for initial overwinding in terms of only the material parameters can be computed to be $\epsilon \hat{\mathbf{u}} \cdot (\mathbf{K}\hat{\mathbf{u}} \times \mathbf{h}) > 0$, where $\mathbf{h} = (-K_1 \hat{u}_2, K_2 \hat{u}_1, K_{23} \hat{u}_1 - K_{13} \hat{u}_2)$.

Effective constitutive laws.—The fact that helices under pure axial force can either over- or underwind is a simple manifestation of the nonlinear response of helical structures under loads. In particular, while the constitutive relations (6) are linear, both the geometry of the helices and the balance laws (4) and (5) are nonlinear. Nevertheless, it is possible to develop an effective linear response theory close to any given helical equilibrium via an appropriate Taylor expansion. Specifically, select a particular helical equilibrium $\mathbf{u}^*$ lying on the hyperboloid, and denote all associated quantities at this equilibrium as M^*, N^*, etc. Then, the linearization of the wrench (M, N) as a function of the strains leads to a linear response relation of the form

$$\begin{bmatrix} M \\ N \end{bmatrix} = \begin{bmatrix} M^* \\ N^* \end{bmatrix} + \begin{bmatrix} A^* & B^* \\ B^* & C^* \end{bmatrix} \begin{bmatrix} \theta \\ z \end{bmatrix}, \qquad (11)$$

where $\theta = |\mathbf{u}| - |\mathbf{u}^*|$, and $z = u_3/|\mathbf{u}| - u_3^*/|\mathbf{u}^*|$. A notable point is that the coefficient matrix is always symmetric and is positive definite, at least in a neighborhood of the unstressed state $\hat{\mathbf{u}}$, and so can be regarded as an effective stiffness matrix. The coefficients A^*, B^*, and C^* are lengthy but explicit expressions of the material coefficients and the equilibrium values as described in the Supplemental Material [16]. Accordingly, for small displacements around any equilibrium helical solution, one can replace the helical structure by a simplified, effectively cylindrical, structure whose configuration is given by the two displacements θ and z, and with the effective energy

$$E = E^* + (M^* - M)\theta + (N^* - N)z$$
$$+ \frac{1}{2}(A^*\theta^2 + 2B^*z\theta + C^*z^2). \qquad (12)$$

The first term is the total energy of the system at the configuration $\mathbf{u}^*$, the second and third terms are work associated with the increments in loads and displacements from $\mathbf{u}^*$, and the quadratic form in the displacements is the elastic energy of the effective system. This effective energy is an extension to general equilibria of the effective energy (1), with the main difference being that the coefficients A^*, B^*, and C^* depend on the equilibrium $\mathbf{u}^*$, or equivalently, the overall load applied to the system. This behavior is routinely reported in experiments, where it is observed that the effective moduli of DNA vary with force [17]. In the particular experiment with no axial torque, the coefficients B^* will change sign as the spring inverts its winding, leading to the observed nonmonotonic behavior. Note also that this effective energy can provide a reasonable approximation to the statistical mechanics of the system close to $\mathbf{u}^*$, provided that the system is in the regime of relatively high tensile loads where fluctuations of the DNA due to interaction with the solvent can reasonably be neglected. Finally, we remark that provided the coefficient matrix in Eq. (11) satisfies appropriate invertibility conditions, the energy (12) can be regarded as a function of any two of the four variables (M, N, θ, z), in order to model experiments where soft, hard, or hybrid loadings are applied.

We remark that experiments will only access helical equilibria that are stable in an appropriate sense. For the purposes of statistical mechanics, the appropriate notion of stability is whether a specific equilibrium is in fact a local minimum of the associated total energy, which in turn depends on the precise form of loading. In the case of complete hard loading, where the orientation and location of each end are controlled, the isoperimetric conjugate point tests for elastic rods, as described in Ref. [18], can be applied to the case of helical equilibria. Each point on the hyperboloid in Fig. 3 corresponds to a helical equilibrium of arbitrary length, and it is a standard result of the calculus of variations that for fully clamped boundary conditions, any sufficiently short helical segment will be a local minimum. For each point on the hyperboloid, the conjugate point computation can be numerically implemented to compute a critical length (possibly infinite), beyond which the equilibrium ceases to be a local minimum, but we are unaware of any simple general characterization of the critical length.

This Letter provides a systematic way to construct two-dimensional effective energies for tweezer experiments when the underlying polymer constitutive relations are known. In particular, it identifies the source of nonmonotonic behavior in simple wrench experiments. Given the geometric framework constructed here, a natural next step is to consider the inverse problem of extracting approximations to the constitutive relations (6) from sets of measurements of the four effective coarse-grain axial load and displacement variables.

[1] J. Gore, Z. Bryant, M. Nöllmann, M. Le, N. Cozzarelli, and C. Bustamante, Nature (London) **442**, 836 (2006).

[2] T. Lionnet, S. Joubaud, R. Lavery, D. Bensimon, and V. Croquette, Phys. Rev. Lett. **96**, 178102 (2006).

[3] J. W. Miller, Jr., Phys. Rev. **14**, 129 (1902).

[4] P. Roelofsen, Recueil Trav. Bot. Neerl. **42**, 72 (1950).

[5] H. Buschmann, M. Hauptmann, D. Niessing, C. Lloyd, and A. Schäffner, Plant Cell **21**, 2090 (2009).

[6] A. Goriely and M. Tabor, Phys. Rev. Lett. **106**, 138103 (2011).

[7] C. Lloyd and J. Chan, Plant Cell **14**, 2319 (2002).

[8] J. Marko, Europhys. Lett. **38**, 183 (1997).

[9] R. Kamien, T. Lubensky, P. Nelson, and C. O'Hern, Europhys. Lett. **38**, 237 (1997).

[10] W. T. Thomson and P. G. Tait, *Treatise on Natural Philosophy* (Cambridge University Press, Cambridge, England, 1867).

[11] A. E. H. Love, *A Treatise on the Mathematical Theory of Elasticity* (Dover, New York, 2013), 4th ed.

[12] N. Chouaieb and J. H. Maddocks, J. Elast. **77**, 221 (2005).

[13] N. Chouaieb, A. Goriely, and J. H. Maddocks, Proc. Natl. Acad. Sci. U.S.A. **103**, 9398 (2006).

[14] S. S. Antman, *Nonlinear Problems of Elasticity* (Springer-Verlag, New York, 1995).

[15] T. McMillen and A. Goriely, J. Nonlinear Sci. **12**, 241 (2002).

[16] See Supplemental Material at http://link.aps.org/supplemental/10.1103/PhysRevLett.111.108103 for computation of the general form of the reduced quadratic energy and an explanation on the geometry of helices in 3D and in curvature space.

[17] F. Mosconi, J. F. Allemand, D. Bensimon, and V. Croquette, Phys. Rev. Lett. **102**, 78 301 (2009).

[18] R. Manning, K. Rogers, and J. Maddocks, Proc. R. Soc. A **454**, 3047 (1998).